

Di-photon decay of a light Higgs state in the BLSSM

Ahmed Ali Abdelalim,^{1,*} Biswaranjan Das,^{1,2,†} Shaaban Khalil,^{1,‡} and Stefano Moretti^{3,§}

¹*Center for Fundamental Physics, Zewail City of Science and Technology,
6 October City, Giza 12588, Egypt*

²*East African Institute for Fundamental Research (ICTP-EAIFR),
University of Rwanda, Kigali, Rwanda*

³*School of Physics and Astronomy, University of Southampton,
Southampton, SO17 1BJ, United Kingdom*

In the context of the $B - L$ Supersymmetric Standard Model (BLSSM), we investigate the consistency of a light Higgs boson, with mass around $90 - 95$ GeV, with the results of a search performed by the CMS collaboration in the di-photon channel at the integrated luminosity of 35.9 fb^{-1} and $\sqrt{s} = 13 \text{ TeV}$.

I. INTRODUCTION

The discovery of a Higgs boson compatible with the one predicted by the Standard Model (SM), h , with a mass of 125 GeV, at the Large Hadron Collider (LHC) in July 2012, has been considered as the beginning of a new era in particle physics. In fact, such a Higgs boson is the first fundamental (i.e., point-like) scalar particle (i.e., with spin 0 and CP-even) to be found in Nature and the last hitherto undiscovered object needed to complete the experimental verification of the SM. This detection confirmed the Higgs mechanism of Electro-Weak Symmetry Breaking (EWSB) generating masses for fundamental particles. It also boosted the expectation of discovering New Physics (NP) Beyond the SM (BSM), as we also know that for, the aforementioned mass value, the SM is theoretically inconsistent. Many of the SM flaws (e.g., the hierarchy problem, the absence of coupling unification, etc.) can however be remedied by Supersymmetry (SUSY), although the latter has itself drawbacks (e.g., the μ problem, the poor consistency of a unified version of it with both collider and Dark Matter (DM) data, etc.) if formulated in its minimal version, the so-called Minimal Supersymmetric Standard Model (MSSM). However, non-minimal realisations of SUSY, e.g., with an enlarged gauge and/or Higgs sector, are both theoretically plausible and better compatible with experimental data [1].

The statistically most significant channel leading to the 2012 signal emerged in the $gg \rightarrow h \rightarrow \gamma\gamma$ production and decay mode, primarily thanks to the high experimental resolution that can be achieved (in the invariant mass of the two photons, $M_{\gamma\gamma}$) via the di-photon final state. Hence, it is not surprising that this channel is being routinely used by ATLAS and CMS in their search for additional (neutral) Higgs bosons, an endeavour that has indeed started immediately after the aforementioned discovery, since most BSM scenarios (Supersymmetric and

not) predict the existence of extra neutral Higgs states. The possibility of the existence of the latter, lighter or heavier than the SM state, thus is an open and challenging phenomenological problem.

The CMS collaboration has recently found potential signals for another neutral Higgs boson, h' , with a mass of 90 to 95 GeV, precisely in the discussed gluon-fusion initiated channel leading to the di-photon final state, i.e., $gg \rightarrow h' \rightarrow \gamma\gamma$. The corresponding data were collected at Center-of-Mass (CM) energies of $\sqrt{s} = 8$ and 13 TeV and integrated luminosities of 19.7 and 35.9 fb^{-1} , respectively [2]. Based on these data, the CMS collaboration observed a resonant structure at $90 - 95 \text{ GeV}$ in the $M_{\gamma\gamma}$ spectrum with a local (global) significance of 2.8 (1.3) standard deviations, respectively. Despite the fact that this hint for a new resonance is still very preliminary, it has gained some attention in the particle physics community and several BSM explanations for it have been proposed [3]. If these observations are confirmed by future data, it will be a significant direct evidence of NP.

In the present paper we show that a specific extension of the MSSM, the the so-called $B - L$ Supersymmetric SM (BLSSM) [4] which has a rich Higgs sector, consisting of two Higgs doublets and two Higgs singlets, can accommodate the observed anomaly. In particular, we emphasize that one of the CP-even Higgs bosons of this BSM construct can act as the potential h' state behind the aforementioned excess in $M_{\gamma\gamma}$, with the model still providing a SM-like Higgs state with 125 GeV, thus compatible with current LHC measurements. The BLSSM is an extension of the MSSM obtained by adopting an additional $U(1)_{B-L}$ gauge group, i.e., the full gauge structure is $SU(3)_C \times SU(2)_L \times U(1)_Y \times U(1)_{B-L}$. This model contains three SM singlet chiral superfields $\hat{N}_{1,2,3}$ (yielding right-handed neutrinos), two SM singlet chiral Higgs superfields $\hat{\chi}_{1,2}$ (providing three additional physical Higgs states) and the \hat{Z}' vector superfield associated with the $U(1)_{B-L}$ gauge boson (embedding a physical Z' state), in addition to the MSSM superfields. Interestingly, it was shown that the scale of $B - L$ symmetry breaking is related to the soft SUSY-breaking scale [5], so that it is not unreasonable to find that this model can predict right-handed neutrinos, Z' and Higgs states at or even

*Electronic address: aabdelalim@zewailcity.edu.eg

†Electronic address: bdas@zewailcity.edu.eg

‡Electronic address: skhalil@zewailcity.edu.eg

§Electronic address: S.Moretti@soton.ac.uk

below the TeV scale.

The mixing between the SM-like Higgs state h and the BLSSM-specific Higgs state h' is proportional to the gauge coupling of the gauge kinetic mixing \tilde{g} between the Z and Z' , which is (in a non-universal description) a free parameter and can be of order of 0.5. In this case, a large Higgs mixing is generated, which yields significant couplings between the h' and SM fermions and gauge bosons. Therefore, the production and decay rates of the h' state are not generally suppressed, including in the $gg \rightarrow h' \rightarrow \gamma\gamma$ channel, which proceeds mainly via top quark and W^\pm gauge boson loops at production and decay level, respectively. Hence, the BLSSM can account for the observed 90–95 GeV potential signal.

The paper is organised as follows. In Sec. II, we describe the Higgs sector of the BLSSM and emphasize that the mass of the lightest CP-even Higgs boson can naturally be around 90–95 GeV with also a SM-like Higgs state having a mass of 125 GeV. In Sec. III, we investigate the would be BLSSM signal in the $gg \rightarrow h' \rightarrow \gamma\gamma$ channel and show that it can explain the excesses presently observed by the CMS collaboration as well as offer a chance for h' discovery already with the full Run 2 data set. Our conclusions are presented in Sec. IV.

II. THE BLSSM HIGGS SECTOR

The BLSSM superpotential is given by

$$W_{\text{BLSSM}} = y_u \hat{Q} \hat{H}_2 \hat{U}^c + y_d \hat{Q} \hat{H}_1 \hat{D}^c + y_e \hat{L} \hat{H}_1 \hat{E}^c + \mu \hat{H}_1 \hat{H}_2 + y_\nu \hat{L} \hat{H}_2 \hat{N}^c + y_N \hat{N}^c \hat{\chi}_1 \hat{N}^c + \mu' \hat{\chi}_1 \hat{\chi}_2, \quad (1)$$

where the first four terms are the usual MSSM ones, the next two terms represent the Yukawa interactions of the known neutrinos and between the additional right-handed ones N_i ($i = 1, 2, 3$) and the singlet Higgs field χ_1 , respectively. The last term represents the bilinear mixing between χ_1 and χ_2 . y_u , y_d , y_e and y_ν are the quark, lepton and neutrino Yukawa coupling constants, respectively. Furthermore, y_N is the the Yukawa coupling constant between N_i and χ_1 , Q and L are the left-handed quark and lepton doublet superfields while U , D and E are the right-handed up-type, down-type and electron-type singlet ones, respectively. The charge conjugation is denoted by the superscript c . Then, H_1 and H_2 are the $SU(2)_L$ Higgs doublet superfields with opposite hypercharge $Y = \pm 1$.

One obtains the masses of the physical neutral BLSSM Higgs states in terms of the Higgs fields,

$$H_{1,2}^0 = \frac{1}{\sqrt{2}}(v_{1,2} + \sigma_{1,2} + i\phi_{1,2}), \quad \chi_{1,2}^0 = \frac{1}{\sqrt{2}}(v'_{1,2} + \sigma'_{1,2} + i\phi'_{1,2}), \quad (2)$$

where the real and imaginary parts correspond to the CP-even (or scalar) and the CP-odd (or pseudoscalar) Higgs

states. $v_{1,2}$ and $v'_{1,2}$ are the Vacuum Expectation Values (VEVs) of the Higgs fields $H_{1,2}$ and $\chi_{1,2}$, respectively. The CP-odd neutral Higgs mass-squared matrix at the tree-level in the basis $(\phi_1, \phi_2, \phi'_1, \phi'_2)$ is given by

$$\mathcal{A}^2 = \begin{pmatrix} B_\mu \tan\beta & B_\mu & 0 & 0 \\ B_\mu & B_\mu \cot\beta & 0 & 0 \\ 0 & 0 & B_{\mu'} \tan\beta' & B_{\mu'} \\ 0 & 0 & B_{\mu'} & B_{\mu'} \cot\beta' \end{pmatrix}, \quad (3)$$

with

$$\begin{aligned} B_\mu &= -\frac{1}{8} \left\{ -2\tilde{g}g_{BL}v'^2 \cos 2\beta' + 4M_{H_1}^2 - 4M_{H_2}^2 \right. \\ &\quad \left. + (g_1^2 + \tilde{g}^2 + g_2^2)v^2 \cos 2\beta \right\} \tan 2\beta, \\ B_{\mu'} &= -\frac{1}{4} \left(-2g_{BL}^2 v'^2 \cos 2\beta' + 2M_{\chi_1}^2 - 2M_{\chi_2}^2 \right. \\ &\quad \left. + \tilde{g}g_{BL}v^2 \cos 2\beta \right) \tan 2\beta', \end{aligned} \quad (4)$$

where $\tan\beta = \frac{v_2}{v_1}$ and $\tan\beta' = \frac{v'_2}{v'_1}$. g_{BL} is the gauge coupling constant of $U(1)_{B-L}$ and \tilde{g} is the gauge coupling constant of the mixing between $U(1)_Y$ and $U(1)_{B-L}$. g_1 and g_2 are the $U(1)_Y$ and $SU(2)_L$ gauge coupling constants, respectively.

The CP-even neutral Higgs mass-squared matrix at the tree-level in the basis $(\sigma_1, \sigma_2, \sigma'_1, \sigma'_2)$ is given by

$$\mathcal{M}^2 = \begin{pmatrix} \mathcal{M}_{hH}^2 & \mathcal{M}_{hh'}^2 \\ (\mathcal{M}_{hh'}^2)^T & \mathcal{M}_{h'H'}^2 \end{pmatrix}, \quad (5)$$

where \mathcal{M}_{hH} is the MSSM CP-even mass matrix which results into a SM-like Higgs boson h with a mass $m_h \sim 125$ GeV and a heavy Higgs boson H with a mass $m_H \sim \mathcal{O}(1)$ TeV. The BLSSM mass matrix $\mathcal{M}_{h'H'}$ reads

$$\mathcal{M}_{h'H'}^2 = \begin{pmatrix} m_{A'}^2 c_{\beta'}^2 + g_{BL}^2 v_1'^2 & -\frac{1}{2} m_{A'}^2 s_{2\beta'} - g_{BL}^2 v'_1 v'_2 \\ -\frac{1}{2} m_{A'}^2 s_{2\beta'} - g_{BL}^2 v'_1 v'_2 & m_{A'}^2 s_{\beta'}^2 + g_{BL}^2 v_2'^2 \end{pmatrix} \quad (6)$$

with $c_x = \cos x$ and $s_x = \sin x$.

The CP-even physical Higgs mass states can be obtained by diagonalising the Higgs mass-squared matrix given by Eq. (5) with a unitary matrix \mathcal{R} as follows:

$$\mathcal{R} \mathcal{M}^2 \mathcal{R}^\dagger = \text{diag}\{m_h^2, m_{h'}^2, m_H^2, m_{H'}^2\}. \quad (7)$$

In order to find solutions consistent with the CMS observation of a scalar of mass around 90–95 GeV [2], we perform a parameter space scan in the BLSSM with an in-house scanning tool which calls the public spectrum generator **SPheno-v4.0.4** [6] to generate the particle spectrum for each randomly scanned parameter space point. **SPheno** requires the model files to generate the output spectrum in the context of a particular model (in our case it is the BLSSM)

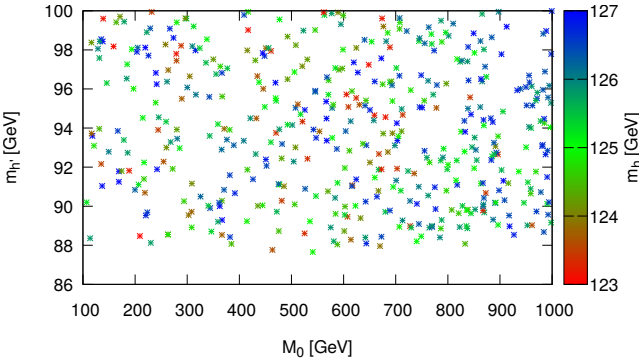


FIG. 1: Scan of $m_{h'}$ vs M_0 with m_h as a colour map.

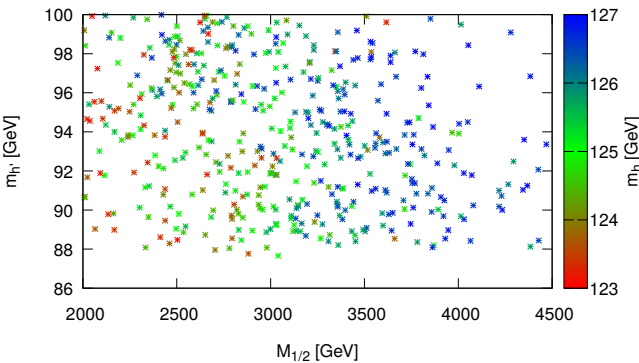


FIG. 2: Scan of $m_{h'}$ vs $M_{1/2}$ with m_h as a colour map.

for a given point. These model files are generated with the public package **SARAH-v4.14.3** [7]. We perform the scan at the GUT scale by varying four input parameters, namely, the universal Soft SUSY-Breaking (SSB) scalar mass term M_0 ($= M_{Q_{1,2,3}} = M_{U_{1,2,3}} = M_{D_{1,2,3}} = M_{L_{1,2,3}} = M_{E_{1,2,3}}$), the universal SSB gaugino mass term $M_{1/2}$ ($= 2M_1 = M_2 = \frac{1}{3}M_3$), $\tan\beta$ and the universal Higgs to sfermion trilinear coupling A_0 ($= A_{\tilde{t}} = A_{\tilde{b}} = A_{\tilde{\tau}}$), while keeping all other model parameters fixed, e.g., $m_{Z'} = 2500$ GeV, $\tan\beta' = 1.15$ and $\mu = \mu' = B_\mu = B_{\mu'} = 0$. The ranges for the variable input parameters are given in Tab. I.

The randomly scanned points are required to produce the lightest neutral Higgs boson mass in the range $90 \text{ GeV} \geq m_{h'} \geq 95 \text{ GeV}$ (approximately). As far as the experimental constraints are concerned, these points should also result in a SM-like Higgs boson with a mass m_h which allows ± 2

Parameter	Range
M_0	$100 - 1000$ GeV
$M_{1/2}$	$1000 - 4500$ GeV
$\tan\beta$	$1 - 60$
A_0	$1000 - 4000$ GeV

TABLE I: Ranges for the four variable input parameters.

BP	$m_{h'}$	m_h	$\sigma(pp \rightarrow h' \rightarrow \gamma\gamma)$	$\sigma(pp \rightarrow h \rightarrow \gamma\gamma)$
1	95.3	125.9	13.1	43.5
2	94.2	125.3	8.6	49.3
3	89.7	125.7	9.7	49.3
4	90.0	127.2	8.7	47.6

TABLE II: The masses (in GeV) of the two lightest neutral Higgs bosons and the cross sections (in fb) at 13 TeV for the processes $pp \rightarrow h' \rightarrow \gamma\gamma$ and $pp \rightarrow h \rightarrow \gamma\gamma$ for the BPs presented in Sec. III.

GeV uncertainty in its theoretical model prediction, about the experimental measurement of $m_h = 125.09 \pm 0.32$ GeV [8]. Moreover, the points are passed through **HiggsBounds-v4.3.1** [9] and **HiggsSignals-v1.4.0** [10] to be consistent with the Higgs boson experimental measurements performed by the LEP, TeVatron and the LHC. **SPheno** also calculates flavour observables, so that the scanned points also need to satisfy the experimental constraints on the Branching Ratios (BRs) of the most stringent B -meson decay channels within a 2σ error, which are given by $\text{BR}(B \rightarrow X_s \gamma) = (3.32 \pm 0.15) \times 10^{-4}$, $\text{BR}(B_s \rightarrow \mu^+ \mu^-) = (3.1 \pm 0.6) \times 10^{-9}$ and $\text{BR}(B_u \rightarrow \tau^\pm \nu_\tau) = (1.06 \pm 0.19) \times 10^{-4}$ [11].

In Fig. 1 we present our randomly scanned points on the $M_0 - m_{h'}$ plane where the colour map represents the values of m_h for those points. It shows a good possibility of having BLSSM solutions with a light scalar state of mass of $90 - 95$ GeV and a SM-like scalar with a mass near 125 GeV, at the same time. Similarly, Fig. 2 depicts the scanned points on the $M_{1/2} - m_{h'}$ plane while the colour map shows the values of m_h . Note that the points with $M_{1/2} < 2000$ GeV are excluded by **HiggsBounds**.

In the next section, we present our Monte Carlo (MC) analysis in the light of the CMS observation of a light scalar in terms of a few Benchmark Points (BPs) selected from our random scan. The details of these BPs are listed in Tab. II. Note that the tabulated cross sections (given at 13 TeV) are calculated with the public package **MadGraph5-v1.5.1** [12], which is also used for our (irreducible) background, i.e., $q\bar{q}, gg \rightarrow \gamma\gamma$ ¹. The ensuing Leading Order (LO) results are supplemented by inclusive k -factors for both signals and background, as follows. We consider the Next-to-LO (NLO) k -factor which is defined as $k_{\text{NLO}} = \frac{\sigma_{\text{NLO}}}{\sigma_{\text{LO}}}$. For the signal, in order to estimate k_{NLO} , we calculate $\sigma(gg \rightarrow h, h')$ both at both LO and NLO using the public tool **SusHi-v1.7.0** [13], since here the largest higher order corrections are only associated with the production process. Here, the value of k_{NLO} is essentially 2.4 in the entire mass range $90 - 125$ GeV. For the background, we assume a constant $k_{\text{NLO}} = 1.3$ in our analysis, following Ref. [14].

¹ As the majority of the excess in the CMS analysis comes from the higher energy data, henceforth, we neglect benchmarking against the 8 TeV ones.

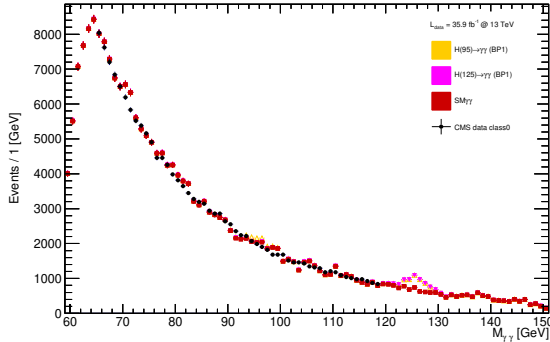


FIG. 3: BP1 versus CMS data at 13 TeV [2]. Yellow points represent $h' \rightarrow \gamma\gamma$, pink points represent $h \rightarrow \gamma\gamma$ while red points show the SM background.

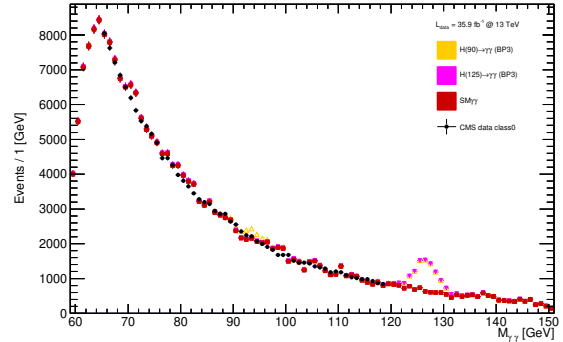


FIG. 5: BP3 versus CMS data at 13 TeV [2]. Yellow points represent $h' \rightarrow \gamma\gamma$, pink points represent $h \rightarrow \gamma\gamma$ while red points show the SM background.

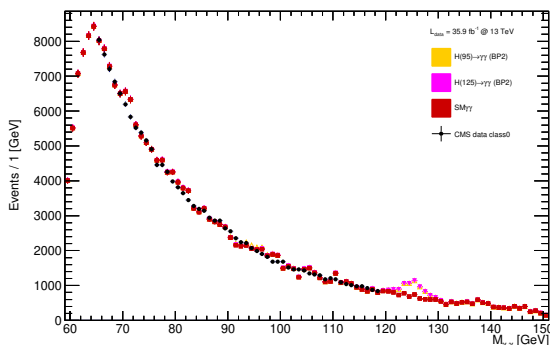


FIG. 4: BP2 versus CMS data at 13 TeV [2]. Yellow points represent $h' \rightarrow \gamma\gamma$, pink points represent $h \rightarrow \gamma\gamma$ while red points show the SM background.

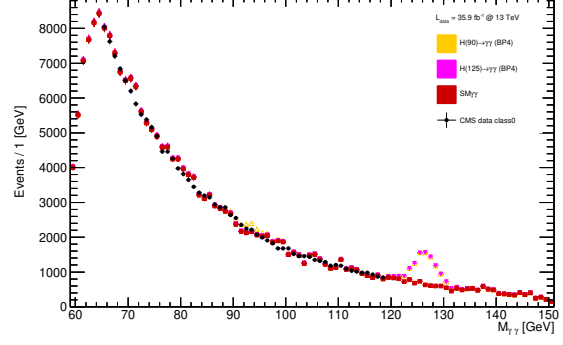


FIG. 6: BP4 versus CMS data at 13 TeV [2]. Yellow points represent $h' \rightarrow \gamma\gamma$, pink points represent $h \rightarrow \gamma\gamma$ while red points show the SM background.

III. NUMERICAL ANALYSIS AND RESULTS

In our analysis, we selected all events that contain a di-photon pair in the detector fiducial range $|\eta^\gamma| \leq 2.5$ and out of the crack region between the barrel and end-cap parts of the CMS Electro-Magnetic (EM) calorimeters. Each photon in the pair has to satisfy a requirement on the ratio of its $p_T^{\gamma i}$ ($i = 1, 2$, with 1(2) being the most(least) energetic one) value to the invariant mass of the di-photon system. These requirements are $p_T^{\gamma 1}/M_{\gamma\gamma} > 30.6/65.0 = 0.47$ and $p_T^{\gamma 2}/M_{\gamma\gamma} > 18.2/65.0 = 0.28$. Our results are therefore directly comparable to the CMS class0 data of [2], which apply the same requirements on the di-photon system. We have digitised such data (see black cross symbols thereafter). Fig. 3–4(5–6) shows the $M_{\gamma\gamma}$ distribution for the aforementioned CMS data (at 13 TeV) alongside the MC ones for our BP1–2(BP3–4), where yellow markers refer to the h' signal, pink markers refer to the h signal while red markers refer to the SM background (the former two being stacked onto the latter). In Figs. 3–4(5–6), we see moderate peaks stemming from the background for the h' signals around 95(90) GeV and clear peaks for the h ones around 125 GeV. To convince

Range of $M_{\gamma\gamma}$ [GeV]	[65-119]	[85-100]	[92-98]	[89-98]
CMS data	170019	38159	14608	22654
SM	171337	37986	14414	22202
h' (BP1)	726	605	536	—
h (BP1)	549	167	72	—
$h' + h + \text{SM}$ (BP1)	172612	38758	15022	—
h' (BP2)	472	396	356	—
h (BP2)	633	192	82	—
$h' + h + \text{SM}$ (BP2)	172442	38574	14852	—
h' (BP3)	1421	1196	—	1150
h (BP3)	1380	419	—	261
$h' + h + \text{SM}$ (BP3)	174138	39601	—	23613
h' (BP4)	1305	1098	—	1057
h (BP4)	1422	431	—	266
$h' + h + \text{SM}$ (BP4)	174064	39515	—	23525

TABLE III: Number of events in the CMS data of [2] and our MC samples in different $M_{\gamma\gamma}$ ranges. Note that the empty cells in the table were not used in the significance calculation.

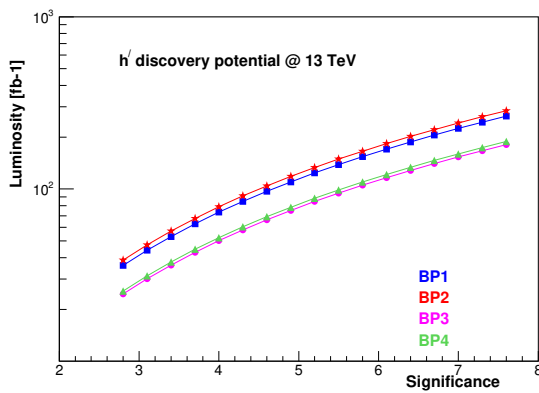


FIG. 7: Integrated luminosity needed for h' discovery in the di-photon channel as a function of significance for BP1–4.

oneself of the statistical relevance of both Higgs boson peaks, we present in Tab. III a comparison between the number of events from each signal and background. We used the number of events in the di-photon mass range 92 – 98 GeV (89 – 98 GeV) to calculate the significance for BP1–2(BP3–4). This has been calculated using the formula S/\sqrt{B} , where S is the number of h' events and B is that of background ones.

Finally, Fig. 7 shows the integrated luminosity needed to discover the h' state of the BLSSM in di-photon events using CMS data at 13 TeV for our four BPs. It is clear that, for all of the latter, discovery is within reach of Run 2, as luminos-

ity values of 114(123)[79]{82} fb^{-1} are needed to reach a 5σ excess in the 90 – 95 GeV region for BP1(2)[3]{4}.

IV. CONCLUSIONS

Motivated by a $\sim 2.8\sigma$ excess recorded by the CMS experiment in the di-photon channel at the integrated luminosity of 35.9 fb^{-1} at $\sqrt{s} = 13 \text{ TeV}$ (in fact, with a moderate contribution from 8 TeV data too) around a mass of order 90 – 95 GeV, we have analysed the discovery potential of a light neutral Higgs boson h' available in the context of the BLSSM at Run 2 of the LHC. We considered four BPs and showed that each of these can produce an enhancement of the di-photon cross section in the above mass region through the sub-process $gg \rightarrow h' \rightarrow \gamma\gamma$ compatible with the CMS anomalous data while simultaneously producing the required amount of signal induced in the same channel by the SM-like state of the BLSSM, so as to comply with the di-photon data collected around 125 GeV. We also estimated the required integrated luminosity needed for a 5σ discovery of such h' state in the above channel, which turned out to be less than the total Run 2 data sample, so that we advocate new analyses using the latter.

Acknowledgments

BD acknowledges the financial support provided by ICTP-EAIFR where part of this project was carried out. SM is financed in part through the NExT Institute and STFC Consolidated Grant No. ST/L000296/1.

[1] S. Khalil and S. Moretti, *Supersymmetry Beyond Minimality: from Theory to Experiment* (CRC Press, Taylor & Francis Group, Boca Raton, FL, 2019).

[2] A. M. Sirunyan *et al.* [CMS], Phys. Lett. B **793**, 320 (2019).

[3] T. Biekötter, M. Chakraborti and S. Heinemeyer, arXiv:2003.05422 [hep-ph]; J. A. Aguilar-Saavedra and F. R. Joaquim, Eur. Phys. J. C **80**, no.5, 403 (2020); T. Biekötter, M. Chakraborti and S. Heinemeyer, arXiv:1910.06858 [hep-ph]; J. Cao, X. Jia, Y. Yue, H. Zhou and P. Zhu, Phys. Rev. D **101**, no.5, 055008 (2020); K. Choi, S. H. Im, K. S. Jeong and C. B. Park, Eur. Phys. J. C **79**, no.11, 956 (2019); T. Biekötter, M. Chakraborti and S. Heinemeyer, PoS **CORFU2018**, 015 (2019); T. Biekötter, M. Chakraborti and S. Heinemeyer, Eur. Phys. J. C **80**, no.1, 2 (2020); S. Heinemeyer and T. Stefaniak, PoS **CHARGED2018**, 016 (2019); S. Heinemeyer, Int. J. Mod. Phys. A **33**, no.31, 1844006 (2018).

[4] S. Khalil and S. Moretti, Front. in Phys. **1**, 10 (2013); L. Basso, A. Belyaev, S. Moretti, G. M. Pruna and C. H. Shepherd-Themistocleous, PoS **EPS-HEP2009**, 242 (2009); L. Basso, A. Belyaev, S. Moretti and G. M. Pruna, J. Phys. Conf. Ser. **259**, 012062 (2010); L. Basso, S. Moretti and G. M. Pruna, Phys. Rev. D **83**, 055014 (2011); W. Emam and S. Khalil, Eur. Phys. J. C **52**, 625 (2007); S. Khalil, J. Phys. G **35**, 055001 (2008).

[5] S. Khalil and A. Masiero, Phys. Lett. B **665**, 374 (2008).

[6] W. Porod, Comput. Phys. Commun. **153**, 275 (2003); W. Porod and F. Staub, Comput. Phys. Commun. **183**, 2458 (2012).

[7] F. Staub, Adv. High Energy Phys. **2015**, 840780 (2015).

[8] G. Aad *et al.* [ATLAS and CMS], Phys. Rev. Lett. **114**, 191803 (2015).

[9] P. Bechtle, O. Brein, S. Heinemeyer, G. Weiglein and K. E. Williams, Comput. Phys. Commun. **181**, 138 (2010); P. Bechtle, O. Brein, S. Heinemeyer, G. Weiglein and K. E. Williams, Comput. Phys. Commun. **182**, 2605 (2011); P. Bechtle, O. Brein, S. Heinemeyer, O. Stål, T. Stefaniak, G. Weiglein and K. E. Williams, Eur. Phys. J. C **74**, no.3, 2693 (2014).

[10] P. Bechtle, S. Heinemeyer, O. Stål, T. Stefaniak and G. Weiglein, Eur. Phys. J. C **74**, no.2, 2711 (2014); O. Stål and T. Stefaniak, PoS **EPS-HEP2013**, 314 (2013); P. Bechtle, S. Heinemeyer, O. Stål, T. Stefaniak and G. Weiglein, JHEP **11**, 039 (2014).

[11] Y. S. Amhis *et al.* [HFLAV], arXiv:1909.12524 [hep-ex].

[12] J. Alwall, M. Herquet, F. Maltoni, O. Mattelaer and T. Stelzer, JHEP **06**, 128 (2011).

[13] R. V. Harlander, S. Liebler and H. Mantler, Comput. Phys. Commun. **184**, 1605 (2013).

[14] S. Catani, L. Cieri, D. de Florian, G. Ferrera and M. Grazzini, JHEP **04**, 142 (2018).